ARTICLE IN PRESS

Extreme Mechanics Letters ▮ (▮▮▮▮) ▮▮▮–▮▮▮

Contents lists available at ScienceDirect

Extreme Mechanics Letters

journal homepage: www.elsevier.com/locate/eml

Wide band-gap seismic metastructures

S. Krödel [a,1], N. Thomé [a,b,1], C. Daraio [a,c,*]

[a] Department of Mechanical and Process Engineering, ETH, Zurich, 8092, Switzerland

[b] Department of Mechanics, Ecole Polytechnique, Palaiseau, France

[c] Engineering and Applied Science, California Institute of Technology, Pasadena, CA, 91125, USA

GRAPHICAL ABSTRACT

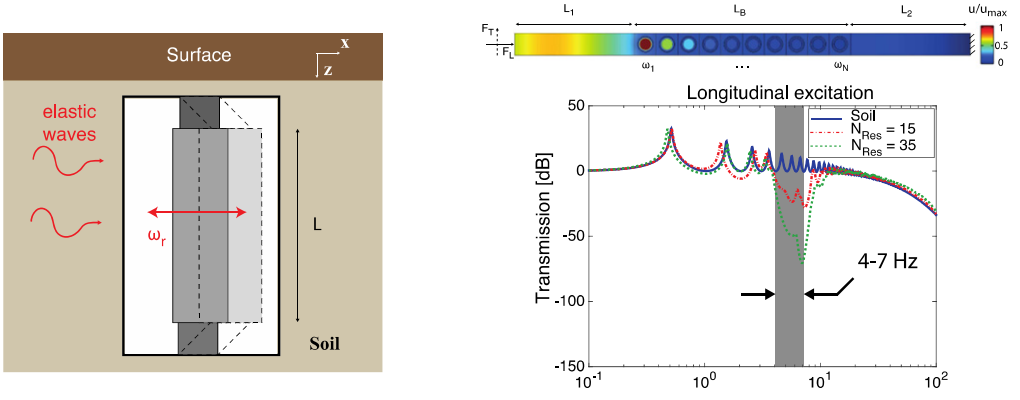

ARTICLE INFO

Article history:
Received 6 April 2015
Received in revised form 27 May 2015
Accepted 27 May 2015
Available online xxxx

Keywords:
Mechanics
Wave-propagation
Metamaterials
Seismic protection
Earthquakes

ABSTRACT

Metamaterials exploit local resonances to reflect acoustic signals with wavelengths well above the characteristic size of the material's structure. This has allowed obtaining materials that present low-frequency (albeit narrow) band gaps or devices for optical and acoustic cloaking. In this work, we propose to use an array of resonating structures (herein termed a "*metastructure*") buried around sensitive buildings to control the propagation of seismic waves. These seismic metastructures consist of arrays of cylindrical tubes containing a resonator suspended by soft bearings. To obtain broadband attenuation characteristics, each resonator in the array is designed to exhibit a different eigenfrequency. We study the response of these systems using numerical analysis and scaled (1:30) experiments. We target wave mitigation in the infrasound regime (1–10 Hz), a range of frequencies relevant for the protection of large buildings.

1. Introduction

The ability to direct the propagation of mechanical waves and to control the transmission spectrum of materials is essential in many engineering applications, ranging

* Correspondence to: Department of Mechanical and Process Engineering, Swiss Federal Institute of Technology Zurich (ETH Zurich), Tannenstr. 3, 8092 Zurich, Switzerland.
E-mail address: daraio@ethz.ch (C. Daraio).

[1] The authors contributed equally to this work.

http://dx.doi.org/10.1016/j.eml.2015.05.004
2352-4316/

Please cite this article in press as: S. Krödel, et al., Wide band-gap seismic metastructures, Extreme Mechanics Letters (2015), http://dx.doi.org/10.1016/j.eml.2015.05.004

from thermoelectrics [1] to sound absorption [2]. Phononic crystals and metamaterials are engineered materials that derive their fundamental properties from the geometry of their structural building blocks, rather than their constituting materials. Phononic crystals rely on the presence of periodicity in their structure, to induce Bragg scattering effects and create band gaps that yield reflections at selected frequency ranges [3]. The first experimental realization of phononic crystals demonstrated the attenuation of sound waves in the audible frequency range by a sculpture [4]. Metamaterials exploit the coupling between propagating waves and local resonances to prevent the propagation of waves at frequencies near resonances. The first realization of metamaterials demonstrated the ability to control electromagnetic waves below the materials' fundamental diffraction limit [5,6]. More recently, research on metamaterials was extended to the design of materials able to control elastic waves, targeting ultrasonic applications in acoustic imaging [7] and acoustic cloaking devices [8,9]. At smaller scales, advances in micro/nanofabrication techniques have allowed the use of metamaterials to control heat by altering high frequency (THz) phonons [10–13]. At very large scales, phononic crystals and metamaterials have been suggested for protecting civil infrastructures from impacts and seismic threats [14–16].

One of the advantages of metamaterials, as compared to phononic crystals, is that metamaterials do not rely on structural periodicity to reflect acoustic waves, and their characteristic sizes can be below the wavelengths of interest. This is particularly relevant for structures that target the reflection of very low frequency waves, for which the use of phononic crystals would require unpractical, large structures. This makes metamaterials particularly interesting in civil engineering application, for example, to shield buildings and civil infrastructures from natural or man-made earthquakes. In these problems, protective materials should be scaled to respond to bulk and surface waves at very low frequencies (1–10 Hz) and large amplitude [17] These low frequencies (i.e., large wavelengths) cannot be controlled by phononic crystals because their size being directly proportional to the wavelength. Being able to design protective structures with characteristic sizes below the natural wavelength makes their fabrication and use accessible with existing construction technologies. Most studies on seismic metamaterials have been theoretical and numerical, and focused on shielding surface waves. Brulé et al. [18] conducted real-size experiments on a seismic phononic crystal consisting of an array of cylindrical holes in the ground. They demonstrated the presence of a phononic band gap around 50 Hz, which is still above the most damaging excitations in a common earthquake spectrum.

Helmholtz-like resonators were also suggested as possible elements to create a seismic shadow zone [19] and as possible solutions to transform elastic wave energy into sound and heat. More recently, an approach that consists of cycloidal resonators that decrease the amplitude of the surface response function has been proposed and analyzed numerically [20]. Metaconcrete, i.e., concrete reinforced with mm-sized coated heavy inclusions, has been proposed to increase the blast mitigation capacity of concrete [21]. Coated heavy inclusions have also been analyzed for vibration isolation of building foundations [22].

2. Materials and methods

In this paper, we propose the use of metastructures to shield sensitive buildings from waves generated by an earthquake. The metastructures consist of arrays of cylindrical, locally resonant units, distributed in the soil surrounding the buildings (Fig. 1(a)). We choose cylindrically shaped resonators due to the widespread use of cylindrical structures in civil engineering (i.e., columns, pipes). This allows a direct translation of the proposed concept in engineering applications. In our proposed systems, the main attenuation of ground excitations arises primarily from the reflection of elastic energy due to the resonant modes of the suspended, rigid cylindrical structures. The metastructures discussed target the mitigation of waves close to the ground surface, however the approach could be extended to protect against bulk waves by placing similar resonating units below the buildings foundations. The resonant units in our proposed metastructures consist of an outer hollow cylinder (for example, a large steel tube, an aluminum hollow cylinder or a concrete pipe, of radius $r_c = 60$ cm with a thickness, $t = 3$ cm) containing a heavy steel mass (a bulk steel cylinder of radius $r_r = 22.5$ cm, length $L = 1.8$ m Young's module $E_r = 210$ GPa, Poisson's ratio $\nu_r = 0.3$ and density $\rho_r = 7850$ kg/m^3 with an overall mass of approximately 2000 kg) suspended between two polymeric springs or bearings (Fig. 1(b)). Variations in the mass of the resonators and/or the stiffness of the suspending springs allow varying the resonator's characteristic eigenfrequency. This particular geometry was selected because it can be constructed with existing building materials and easily adapted to size constraints of different applications. For example, in a full-scale realization of the metastructures, different commercial rubber bearings could be used as soft springs, being already available in variable sizes and stiffness grades [23]. The equivalent spring stiffness k_{RB} of a rubber bearing can be approximated by [23]

$$k_{RB} = G\frac{A}{H}, \tag{1}$$

where G is the shear modulus of the rubber material, A is the area and H is the height of the bearing. The resonance frequency of the resonators can be tuned changing one or more of these three parameters. The resonant mode of interest is depicted in Fig. 1(c), and shows the vibration of the inner rod suspended by the two polymeric springs. Each resonator is envisioned to be buried underground close to or at the ground surface, around the buildings to be protected. In most configurations, the bending frequencies of the inner rod and the structural frequencies of the outer cylinder are much higher than the resonance of the inner mass suspended by the soft springs and play no significant role in the protection of the buildings. Each resonator can be modeled as an equivalent, two-dimensional (2-D), plain strain element in the frequency domain (see Fig. 1(d)). In

Please cite this article in press as: S. Krödel, et al., Wide band-gap seismic metastructures, Extreme Mechanics Letters (2015), http://dx.doi.org/10.1016/j.eml.2015.05.004

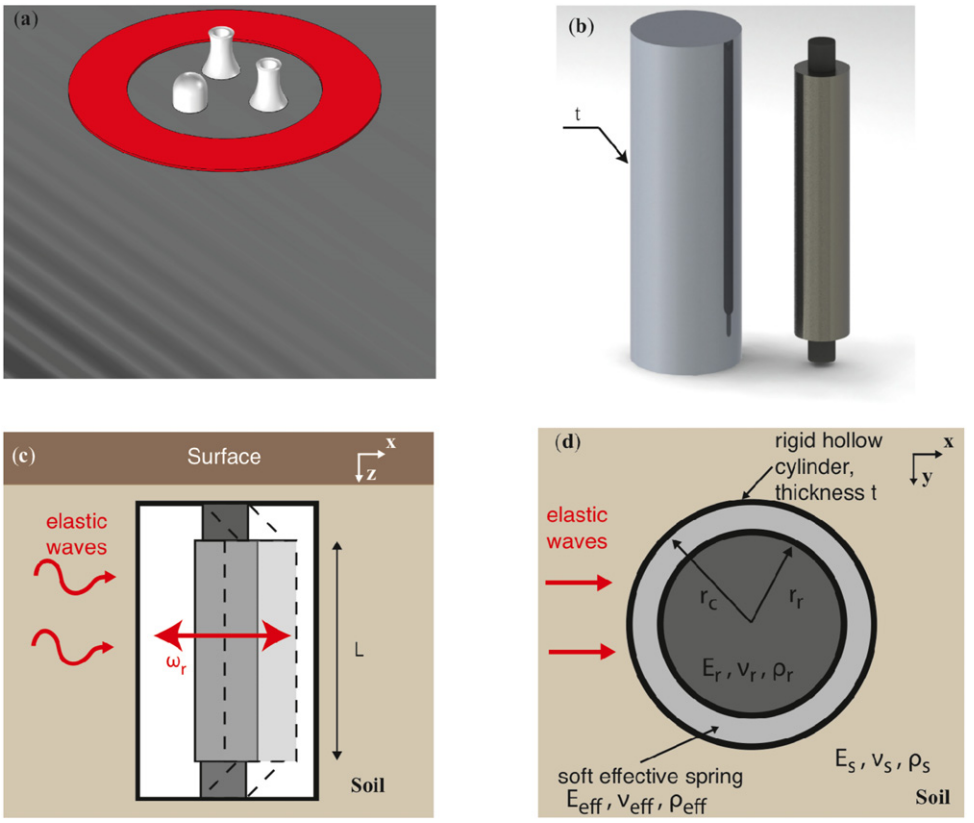

Fig. 1. (a) Schematic diagram showing vulnerable buildings (white structures) that are endangered by an incoming surface wave. The red ring around the buildings represents the area with buried local resonators. (b) Components in a resonator, consisting of a cylindrical hollow tube (left), containing a heavy bulk cylinder (right, shown separately) suspended by polymeric springs (black). (c) Illustration of the assembled resonator and its resonance mode of interest, when embedded into soil. (d) The two-dimensional representation of the system in (c). The springs on top and bottom of the resonator are replaced by an effective surrounding medium, which yields the same eigenfrequency ω_r. (For interpretation of the references to color in this figure legend, the reader is referred to the web version of this article.)

such a 2-D model, a rigid mass (representing the inner rod) is surrounded by an effective continuum material (representing the soft springs), which yields in the same eigenfrequency ω_r.

One draw-back of resonant metamaterials is that band gaps arising from local resonances are confined to a very narrow frequency range, centered around the resonant frequency [7]. This is in sharp contrast with the requirements in civil engineering application, where buildings must be protected from a rather broadband spectrum of a common earthquake. Several approaches have been proposed to widen the band gap of resonant metamaterials, ranging tuned damping [24] to geometries that enhance the effect of localized modes [25]. To attenuate waves in a broader frequency spectrum, we use arrays of resonators composed of units resonating at different frequencies. To achieve a better mode overlap, we space the resonance frequencies ω_1 to ω_N logarithmically between 4 and 7 Hz.

Resonators with distributed resonant frequencies have been proposed earlier in optical [26,27] and acoustic systems [28], and are referred to as "rainbow traps" because they split propagating waves into a spatial spectrum. This principle can be exploited for earthquake excitations, such that every frequency component of the earthquake excites a different spatial region of the barrier, which enhances the barrier's efficiency over a broad frequency region. The rainbow effect is achieved selecting different stiffness in the connecting soft springs.

To validate this concept numerically, we model the transmission of longitudinal and shear waves through an array of resonators (Fig. 2(a)) using the equivalent two-dimensional (2-D) model described in Fig. 1(d). We expect this model to be representative of the response of surface waves in a 3-D scenario. To tune the working frequency of each resonator and create the "rainbow trap" we fix the inner mass (L and r_r) and adapt the effective Young's modulus of the surrounding material ring. We obtain the formula for the effective Young's modulus as a function of the desired eigenfrequency, with an analytical model (see Supplementary Materials in Appendix A):

$$E_{\text{eff}} = \omega_r^2 \frac{r_r^2 \rho_r R^2 (1 - R^2 + 9(1 + R^2)\ln(R))}{12\pi(1 + R^2)}, \qquad (2)$$

where $R = \frac{r_r}{r_c}$. Here, the density is taken to be $\rho_{\text{eff}} = 1225\ \text{kg/m}^3$, which is similar to the density of rubbery elastomers.

We first investigate the influence of the number of resonators on the wave attenuation. We position the resonators 0.9 m apart from each other, starting on the left

Please cite this article in press as: S. Krödel, et al., Wide band-gap seismic metastructures, Extreme Mechanics Letters (2015), http://dx.doi.org/10.1016/j.eml.2015.05.004

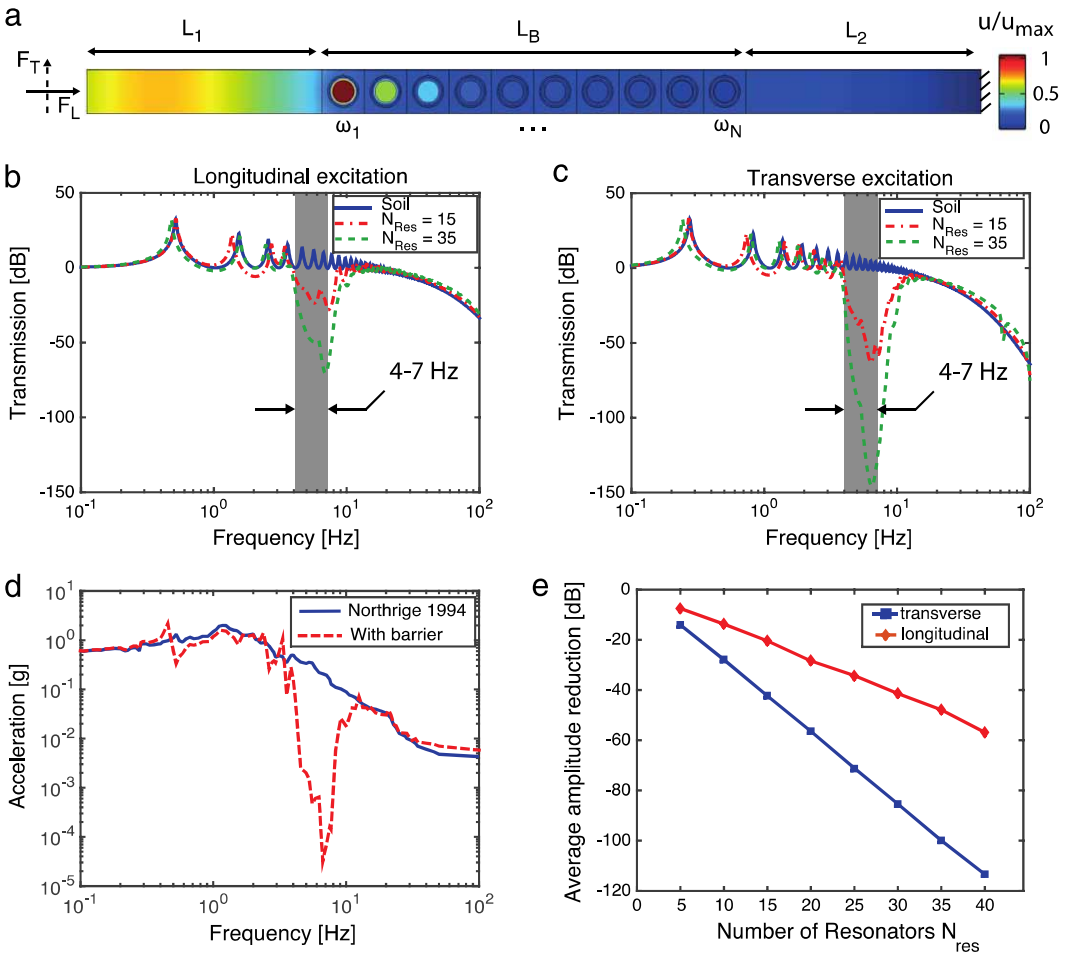

Fig. 2. (a) Schematic diagram of a resonator array in our 2-D equivalent model. The color intensity shows the normalized displacement amplitude. In this case the vibration is localized around resonator ω_1. (b) Transmission spectrum for longitudinal waves ($F_T = 0$) for varying number of resonators (0, 15 and 35). (c) Transmission spectrum for transverse excitations ($F_L = 0$). (d) To show the potential filtering effect for the spectrum of a real earthquake, we apply the transfer function with 35 resonators to the Northridge earthquake from 1994. The earthquake recording data can be downloaded from the PEER Ground Motion Database [29]. (e) Design guideline for the average attenuation as a function of the number of resonators in the array. (For interpretation of the references to color in this figure legend, the reader is referred to the web version of this article.)

with the resonator with the highest resonance frequency (7 Hz), and arrange the remaining resonators in order, following a logarithmically decreasing resonant frequency (i.e., 7.00, 6.73, . . . , 4.16, 4.00 Hz for the case of 15 resonators). However, numerical simulations showed that changes in the resonators' ordering and proximity did not affect the transmission spectrum. We model a system, which consists of a homogeneous soil inlet of length L_1, followed by the seismic barrier with length $L_B = 0.9\,\mathrm{m} * N_{\mathrm{res}}$ and a homogeneous soil outlet of length L_2 (Fig. 2(a)) in Comsol Multiphysics©. To compare results, the total length of the system, $L_T = L_1 + L_2 + L_B = 70$ m, is kept constant, while the length of the barrier (i.e., the number of resonators) changes. This means that for a smaller number of resonators L_1 and L_2 are increasing in the models. We excite shear or longitudinal waves by an oscillating boundary load $F_{L/T}$ on the left side and measure the reaction force on the fixed end on the right side. We define the transmission function of the system T as the ratio between the longitudinal or transversal excitation and the reaction force in x and y, respectively:

$$T = \frac{F_{Rx/Ry}}{F_{L/T}}. \tag{3}$$

We apply periodic boundary conditions to the top and bottom of the domain to avoid boundary effects. Furthermore, we use a linear elastic Young's modulus, $E_S = 20$ MPa, and a Poisson's ratio of 0.3 for the soil. The density is set to $\rho_s = 1300\ \mathrm{kg/m^3}$. To account for damping, we use an isotropic loss factor $\eta_S = 0.03$ for the soil and $\eta_r = 0.1$ for the soft effective material surrounding the resonator mass. In practice, the amount of damping in soil might be higher and frequency dependent [30]. The high damping value chosen for the resonator springs accounts for the fact that most rubber bearings are made of medium or highly dissipative rubber sheets.

3. Results and discussion

In Fig. 2(b,c) we display the results for the transmission of longitudinal and shear waves through homogeneous

Please cite this article in press as: S. Krödel, et al., Wide band-gap seismic metastructures, Extreme Mechanics Letters (2015), http://dx.doi.org/10.1016/j.eml.2015.05.004

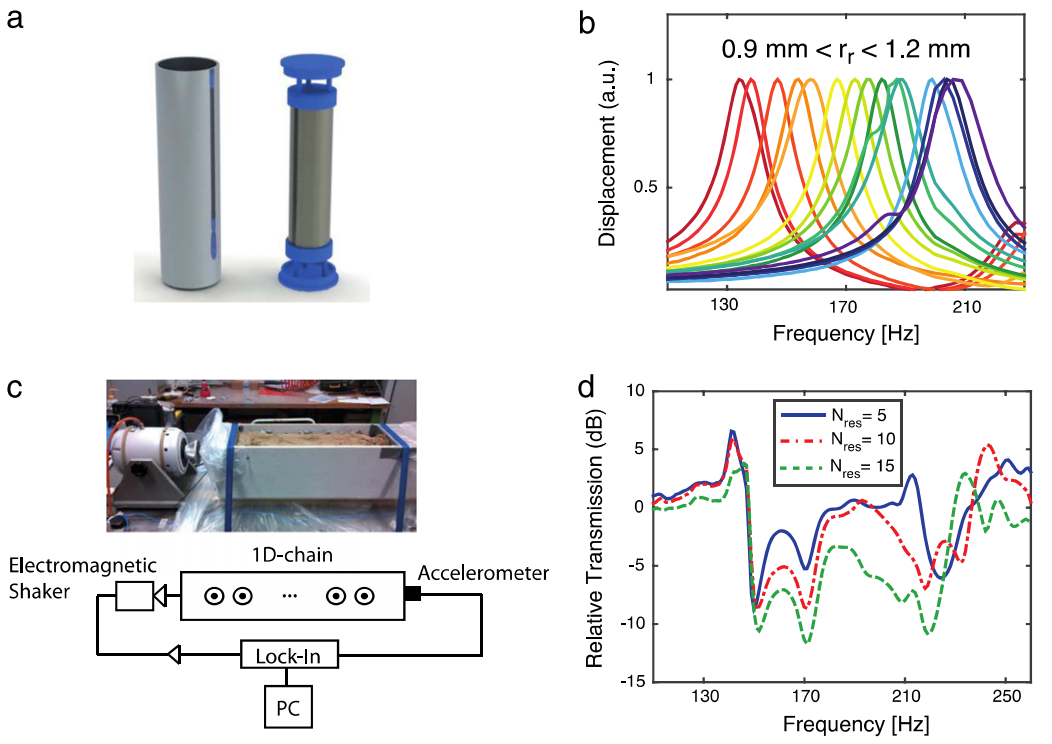

Fig. 3. Experimental setup and results. (a) Scaled design of the resonators. The connecting springs are highlighted in blue. (b) Resonant response of the 15 resonators used in experiments (measured separately). The curves are plotted together to highlight the "rainbow trapping" effect. (c) Digital image of shaker and sand box and_schematic diagram of the setup showing how the resonators are positioned. (d) Transmission curves showing the attenuation provided by the scaled metastructures, as a function of an increasing number of resonators, relative to the transmission through pure sand. (For interpretation of the references to color in this figure legend, the reader is referred to the web version of this article.)

soil ($L_B = 0$), and compare that to the transmission through barriers composed of 15 and 35 resonators. In the frequency region of interest, we observe a clear decrease in transmission of up to −80 dB for the longitudinal and −150 dB for the transversal excitation. The difference between shear and longitudinal attenuation can be explained by the generally higher damping of shear waves. We note that the attenuation effect extends over a slightly larger frequency range than expected. This can be explained by the rather high bandwidth of the resonances at high loss factors. To test how these structures would perform when excited with the signal of a real earthquake, we compare the transfer function obtained with a 35 resonator barrier and the signal transferred across pure soil ($T_B = \frac{T_{N_{Res}=35}}{T_{N_{Res}=0}}$) when the acceleration spectrum of the Northridge earthquake from 1994 (recorded by the Beverly Hills station, 12 520 Mulhol, data can be downloaded from PEER Ground motion database [29]) is used as the excitation signal. Fig. 2(c) shows that the barrier would drastically minimize the acceleration in the dangerous frequency region and function as an efficient shielding mechanism.

We investigate the relation between the amplitude reduction and the total number of resonators, as a design guide for a possible earthquake barrier. In Fig. 2(e) we describe the averaged amplitude reduction in dB as a function of the number of resonators, between 4 and 7 Hz. The average amplitude reduction has been calculated by the following formula for the different number of total resonators:

$$R = \frac{1}{m}\sum_{n=1}^{m} T(n)_{N_{Res}=5,\ldots,40}. \quad (4)$$

In this case, m is the number of discrete frequency steps that have been considered in our model between 4 and 7 Hz. It is important to mention that, in a 3-D scenario, the proposed barrier is expected to reflect surface waves, deflect incoming surface waves in the bulk and also partially store elastic energy. The role of gravity, bulk waves propagation and a more complex three-dimensional geometry of the resonators will be a subject of future studies.

To verify our design concept, we built a 1:30 scaled experimental setup, and tested metastructures with a variable number of resonators. To scale the size and properties of the resonators, we neglect gravity effects and follow the approach for a prototype material [31] (see Supplementary Materials in Appendix A). The design of the resonators for experiments (Fig. 3(a)) follows the scaling laws summarized in Table S1.

In the experiments, we fabricate 15 different resonators varying the design of the spring geometry to vary the resonant frequency, while the inner mass is kept constant. Each resonator in the metastructure consists of an outer aluminum tube, 80 mm long, 1 mm thick and with an external diameter of 22 mm, containing a resonant mass made of a cylindrical steel rod with diameter 15 mm and length

Please cite this article in press as: S. Krödel, et al., Wide band-gap seismic metastructures, Extreme Mechanics Letters (2015), http://dx.doi.org/10.1016/j.eml.2015.05.004

60 mm. The connecting springs (Fig. 3(a), highlighted in blue) have been designed using Solid Works© and have been manufactured with an Objet 3D-printer using the polymeric material Vero Blue, which has a density of approximately 1200 kg/m^3 and a Young's modulus of 1.1 GPa, according to tensile tests carried out in our lab. The spring design consists of a circular base plate, which is connected the mounting plate of the inner mass with thin beam-like elements. The thin beam elements are necessary to provide overall low effective spring stiffness for the mode of interest (see Fig. 1(c)). The base plate is inserted into the outer rigid hollow cylinder. The heavy inner mass is then connected to the mounting plate with a press fit. This also allows removing the cylindrical mass easily and replacing it with another one made of a different material (e.g. aluminum instead of steel), to target different frequencies. The connecting spring stiffness is estimated analytically using a beam model, which also accounts for the elastic deformation of the base plate (see Supplementary Material in Appendix A). To adapt the resonance frequency, we vary the radius of the three connecting beams in the spring structure (see the blue region in Fig. 3(a)) between 0.9 and 1.2 mm. We note that the polymeric springs designed for the scaled down experiments are not expected to withstand dynamic loads equivalent to the one found in civil applications. However, in a full size design of the resonators, they could be replaced by commercially available construction rubber bearings with scaled stiffness.

To characterize each resonator independently, we measure their dynamic response in air, exciting each of them with a piezoelectric actuator on one side and measuring the displacement amplitude of the inner mass with a laser vibrometer (Polytec OFV-534). The normalized response of the 15 resonators fabricated is plotted in Fig. 3(b), where each curve shows the response of a single resonator. The different resonant peaks are plotted next to each other to underline the spreading and overlapping of resonant modes (as in the rainbow trapping effect). In our experiments, the resonant frequencies of the resonators range between 134 and 208 Hz, which represent a real-scale frequency range of 4.46–6.93 Hz.

To measure the collective effect of metastructures constructed with variable number of resonating units, we built a customized testing platform. The experimental setup consists of a glass–ceramic box, 60 cm in length, 22.5 cm wide and 21 cm deep, containing sand as a model material for soil (see Fig. 3(c)). Sand is assumed to be a non-dispersive material, in both the full-scale and small-scale scenarios, as the wavelengths considered are very large compared to the size of the sand particles [32–34]. We do not analyze specific size effects of sand that could influence the interaction between the soil and the resonators. However, we note that wetness and variable stiffness of the soil can affect the response of the metastructure. In our experiments, we monitor the humidity and compaction of the sand to obtain repeatable measurements. To scatter waves and minimize reflections at the box boundaries, we added larger stones and gravel to the sand at the boundaries of the box. We excite bulk waves on one side of the box, near the surface, using and electromagnetic shaker (TIRA, maximum force 200N) attached to a metal plate that can move on an elastic membrane. We measure the transmitted waves using an accelerometer (PCB 356A01), placed on the other side of the box, where we attached the same metal plate on an elastic membrane. The frequency of the excitation signal is swept between 100 and 260 Hz using a lock-in amplifier (Stanford Instruments), to minimize the influence of mechanical noise (Fig. 3(c)). We position the resonators in a single array within the box as shown in Fig. 3(c), and measure the signal transmitted through the sand box as a function of frequency and number of resonators.

We inserted resonators in order, from the lowest to the highest resonant frequency. We began testing first the response of the five resonators with lowest resonant frequencies (i.e., the resonators centered at 134, 138, 147, 153 and 158 Hz) and then repeated the measurements adding five other resonators with the next higher resonant frequencies (i.e., the resonators centered at 167, 173, 177, 183 and 187 Hz). We plot the transmission of the signal obtained with 5, 10 and 15 resonators, relative to the transmission through sand without resonators (Fig. 3(d)). The attenuation of the signal in the expected frequency range is clearly visible even when only five resonators are buried in the sand, and it increases with the number of resonators (reaching a maximum attenuation of −11.7 dB when all 15 resonators are inserted in the sand box). Interestingly, when the number of resonators in the metastructure is small (e.g., when testing only five resonators) we observe a small amplification of the signal, around 210 Hz. We attribute this phenomenon to in-phase coupling of the resonator with the surrounding soil. A similar effect was observed also in the numerical model for a low number of resonators. This undesired amplification could be minimized using a higher number of resonators as seen in Fig. 2(b). When the resonance frequencies of the resonators are more closely spaced, the in phase motion of one frequency is canceled by the out of phase motion of the next, reducing amplification. This effect results in a smoother transmission spectrum within the attenuation zone, where the effect of single resonances is no longer visible. Although the response of the scaled experiments matches the predicted attenuation frequency range, a quantitative comparison with our numerical model is not possible. This is because in the scaled experimental setup boundary reflections cannot be avoided and the coupling between the resonators and the soil is imperfect. In addition, even though the excitation was provided close to the surface of the sand, we could not monitor the surface displacement and, therefore, measure the energy propagating. The results obtained experimentally are not fully transferable to real earthquake scales, because our scaling approach (see Supplementary Materials in Appendix A) neglects gravitational effects and heterogeneities that may be present in real soil or rocks. Furthermore, we did not investigate the effects of materials aging and/or environmental conditions, which should be accounted for in the design of real-scale meta-structures.

4. Conclusion

In summary, we apply the concept of locally resonant metamaterials to attenuate low frequency waves, aiming

Please cite this article in press as: S. Krödel, et al., Wide band-gap seismic metastructures, Extreme Mechanics Letters (2015), http://dx.doi.org/10.1016/j.eml.2015.05.004

at the design of new civil infrastructures (i.e., metastructures) to protect sensitive buildings from earthquake excitations. We show that creating arrays of resonators with distributed resonance frequencies (using the concept of "rainbow traps" in a civil engineering context) can expand absorption to a broader frequency spectrum than other existing approaches. We validate our concept and modeling approach experimentally in a 1:30 scaled system. We propose a resonator geometry for full-scale applications that takes into account construction constraints and availability of conventional construction materials, using commercially available rubber bearings. The resonators proposed are very versatile and can in principle be tailored to a large range of target frequencies. The proposed shielding design could also be easily adapted to fracking and drilling applications. Future analysis should focus on the study of energy localization and dissipation on single and multimode resonators, on the role of gravitational effects, and on modeling three-dimensional wave fields.

Acknowledgments

We acknowledge helpful discussions with Prof. E. Schatzi (ETH Zurich), Prof. B. Stojadinovic (ETH Zurich) and A. Palermo (Univ. of Bologna). Furthermore we acknowledge the assistance of A. Bergamini (ETH Zurich) and J. Tomasina (ETH Zurich) in the development of the experimental setup.

Appendix A. Supplementary materials

Supplementary material related to this article can be found online at http://dx.doi.org/10.1016/j.eml.2015.05.004.

References

[1] G.J. Snyder, E.S. Toberer, Nature Mater. 7 (2008) 105.
[2] C. Zwikker, C.W. Kosten, Sound Absorbing Materials, Elsevier Pub. Co., 1949.
[3] M. Kushwaha, P. Halevi, Phys. Rev. Lett. 71 (1993) 2022.
[4] R. Martínez-Sala, J. Sancho, J.V. Sánchez, V. Gómez, J. Llinares, F. Meseguer, Nature 378 (1995) 241.
[5] J. Pendry, Phys. Rev. Lett. 85 (2000) 3966.
[6] R.a. Shelby, D.R. Smith, S.C. Nemat-Nasser, S. Schultz, Appl. Phys. Lett. 78 (2001) 489.
[7] Z. Liu, X. Zhang, Y. Mao, Y.Y. Zhu, Z. Yang, C.T. Chan, P. Sheng, Science 289 (2000) 1734.
[8] L. Zigoneanu, B. Popa, S. Cummer, Nature Mater. 13 (2014) 1.
[9] N. Stenger, M. Wilhelm, M. Wegener, Phys. Rev. Lett. 108 (2012) 014301.
[10] N. Zen, T.A. Puurtinen, T.J. Isotalo, S. Chaudhuri, I.J. Maasilta, Nature Commun. 5 (2014) 1.
[11] J.-K. Yu, S. Mitrovic, D. Tham, J. Varghese, J.R. Heath, Nat. Nanotechnol. 5 (2010) 718.
[12] P.E. Hopkins, C.M. Reinke, M.F. Su, R.H. Olsson, E. a Shaner, Z.C. Leseman, J.R. Serrano, L.M. Phinney, I. El-Kady, Nano Lett. 11 (2011) 107.
[13] B. Kim, N. Janet, R. Charles, Z.-M. Maryam, I. El-Kady, D. Goettler, M. Su, Z.C. Leseman, R.H. Olsson, ECS Trans. 50 (2012) 449.
[14] Z. Shi, Z. Cheng, H. Xiang, Soil Dyn. Earthq. Eng. 57 (2014) 143.
[15] Z. Shi, Z. Cheng, C. Xiong, Earth Sp. (2010) 2586.
[16] J. Huang, Z. Shi, J. Sound Vib. 332 (2013) 4423.
[17] R.D. Woods, J. Soil Mech. Found. Div. ASCE 94 (1968) 951.
[18] S. Brûlé, E.H. Javelaud, S. Enoch, S. Guenneau, Phys. Rev. Lett. 112 (2014) 133901.
[19] S. Kim, M.P. Das, Modern Phys. Lett. B 27 (2013) 1.
[20] G. Finocchio, O. Casablanca, G. Ricciardi, U. Alibrandi, F. Garescì, M. Chiappini, B. Azzerboni, Appl. Phys. Lett. 104 (2014) 191903.
[21] S.J. Mitchell, A. Pandolfi, M. Ortiz, J. Mech. Phys. Solids 65 (2014) 69.
[22] Z.B. Cheng, Y.Q. Yan, F. Menq, Y.L. Mo, H.J. Xiang, Z.F. Shi, K.H. Stokoe, Proc. World Congr. Eng., vol. III, 2013.
[23] 2014. http://www.bridgestone.com/products/diversified/antiseismic_rubber/.
[24] J.M. Manimala, C.T. Sun, J. Appl. Phys. 115 (2014) 023518.
[25] O.R. Bilal, M.I. Hussein, Appl. Phys. Lett. 103 (2013) 111901.
[26] K.L. Tsakmakidis, A.D. Boardman, O. Hess, Nature 450 (2007) 397.
[27] Q. Gan, Y. Gao, K. Wagner, D. Vezenov, Y.J. Ding, F.J. Bartoli, Proc. Natl. Acad. Sci. USA 108 (2011) 5169.
[28] J. Zhu, Y. Chen, X. Zhu, F.J. Garcia-Vidal, X. Yin, W. Zhang, X. Zhang, Sci. Rep. 3 (2013) 1.
[29] 2015. http://ngawest2.berkeley.edu.
[30] B. Beranek, J. Sound Vib. 49 (1976) 179.
[31] H.G. Harris, G. Sabnis, Structural Modeling and Experimental Techniques, second ed., Taylor & Francis, 1999.
[32] T. Wichtmann, E.I. Sellountos, S.V. Tsinopoulos, A. Niemunis, D. Polyzos, T. Triantafyllidis, D.E. Beskos, 5th GRACM Int. Congr. Comput. Mech., 2005.
[33] C.N. Thomas, S. Papargyri-Beskou, G. Mylonakis, Soil Dyn. Earthq. Eng. 29 (2009) 888.
[34] E.C. Leong, J. Cahyadi, H. Rahardjo, Can. Geotech. J. 46 (2009) 792.